Journal of Applied Sciences

ISSN 1812-5654

science alert

ANSInet
an open access publisher
http://ansinet.com

Journal of Applied Sciences, 6 (4): 911-918, 2006
ISSN 1812-5654
© 2006 Asian Network for Scientific Information

Reducing Load Effects in High-energy, High-efficiency Inductive Links

[1]H. Ghariani, [1]M. Chaoui, [1]M. Lahiani, [2]R. Perdriau and [1]F. Sellami
[1]Ecole Nationale D'ingénieurs De Sfax-Route Sokra Km 4, Bp W 3038 Sfax, Tunisia
Laboratory of Electronics and Information Technologies
[2]Eseo-4, Rue Merlet-de-la-boulaye-B.P., 30926-49009 Angers, France

Abstract: This study deals with an optimization method of the mutual inductance between two magnetically coupled coils of an inductive link, in order to ensure efficient energy and data transmission in implantable electronic devices. Such an approach optimizes the voltage gain and the power yield as a function of the lateral and longitudinal displacements between the external coil (transmitter) and the implanted coil (receiver). The geometry of these coils has to be the least sensitive to displacements and the most stable with respect to mutual inductance. It was created for inductive links with high power transfer capability combined with high overall efficiency. The variations of the reflected impedance are minimized thanks to a rigorous choice of this geometry, which ensures a stable voltage gain for various loads.

Key words: Inductive link, mutual inductance, coil geometries, load effects

INTRODUCTION

Any electronic device requires an adequate power supply for proper operation. Indeed, within the field of micro-implanted devices, this issue becomes more and more topical in terms of functionality. In these devices, maximum energy has to be transmitted from the external part of the implant to the internal one. This is often achieved by the means of an inductive link involving two coils: in order to achieve efficient coupling, mutual inductance is used to link both parts together (Galbraith *et al*., 1987; Chaoui *et al*., 2003a). Therefore, the sensitivity of the mutual inductance to displacements between the internal part and the external part has to be studied in order to obtain the maximum system stability, in spite of lateral displacements caused by a wrong positioning of both coils (Chaoui *et al*., 2003b).

In this study, a novel mathematical analysis of a RF inductive link thus extends existing studies to the case of very low coupling factors. It takes into account the parasitic resistance of the coils, which proves to be critical especially in the case of micro-coils. A geometry is then proposed for both coils in order to enhance the overall power yield of the link, especially relevant in the case of high efficiency requirements compensating for losses in the external transmitter (Soma *et al*., 1987; Chaoui *et al*., 2003c; Muñoz *et al*., 2000).

The variation of the reflected load has a major effect on the system: each coil misalignment yields a different value of the reflected load, while the secondary load itself remains a constant. Consequently, this reflected load can be expressed as a function of longitudinal and lateral displacements.

The coupling factor is generally more suitable as a design parameter thanks to its dependency on the number of coils (the M dependency is in fact cancelled by the Li dependency), thus making the analysis a little bit complex. In any case, the amount of energy transferred to the secondary winding greatly depends on this coupling which ultimately defines the voltage gain, the power yield of the link and the tolerance of the system to lateral and longitudinal misalignments. As a result, it can be shown that the formulation of the voltage gain and the power yield actually depends on lateral and longitudinal displacements rather than on the coupling factor k.

PRINCIPLE OF LOAD EFFECT IN INDUCTIVE LINK

Figure 1 shows a typical voltage-in voltage-out link configuration. It depicts an equivalent circuit of an inductive link for transcutaneous power and data transfer. This link consists of a serial tuned transmitter and a parallel tuned receiver circuit, which are magnetically coupled. Resistor R_1 is the output resistance of the RF-amplifier driving the link, including the resistance which determines the resonant circuit quality factor Q_e. The R_p resistor includes the load and the resistance of the resonant circuit. R_{L1}, R_{L2}, Q_e and Q_r, respectively represent the series resistances of the coils and the quality factors of the transmitter and the receiver.

Corresponding Author: H. Ghariani, Ecole Nationale D'ingénieurs De Sfax-Route Sokra Km 4, BP W 3038 Sfax, Tunisia
Tel: 21674274088 Fax: 21674275595

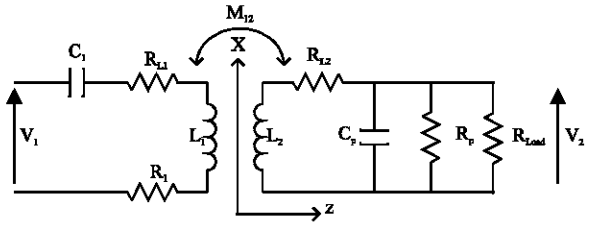

Fig. 1: Generic schematic of a transpo0nder system for power and data transmission

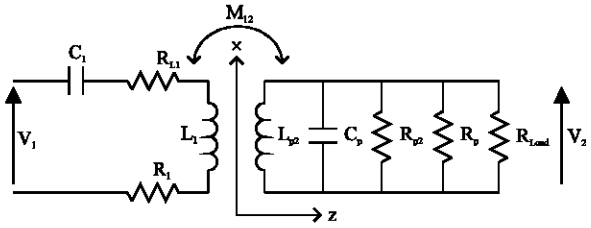

Fig. 2: Approximated circuit of the trasponder system for power and data transmission

For better understanding, the circuit in Fig. 1 is rearranged as shown in Fig. 2.

In which coil losses are represented by the parallel inductor L_{p2} and the parallel resistor R_{p2}. The series and parallel inductance and resistance of the coils are linked together by the following formulae:

$$L_{p2} = L_2 + \frac{R_{L_2}^2}{L_2\omega^2} \quad (1)$$

and

$$R_{p2} = R_{L_2} + \frac{(L_2\omega)^2}{R_{L_2}} \quad (2)$$

R_2 represents the equivalent parallel resistance of R_{p2}, R_p and R_{Load} and is given by

$$R_2 = R_{p2} // R_p // R_{load} \quad (3)$$

and

$$Q_e = \frac{1}{R_{sL1}C_1\omega_1} \quad (4)$$

in which R_{sL1} is the series resistance of R_{L1} and R_1.

A new theoretical analysis of this particular case was performed as an extension of current theoretical studies, adding to the equations the impact of the parasitic resistance of the receiver coil; to do so, a MathCAD program was developed as a tool that helps significantly the RF-link designer. In order to determine the whole quadripole describing the inductive link, the emitter-receiver circuit containing all coupled coils is first evaluated. The L_1 coil is coupled to the L_{p2} coil with a k(z,x) coupling factor. The impedance matrix Z thus becomes (Zierhofer and Hochmair 1990; Catryasse *et al*., 2004):

$$Z = \begin{pmatrix} Z_{11} & Z_{12} \\ Z_{21} & Z_{22} \end{pmatrix} \quad (5)$$

which can be detailed as:

$$Z(f,z,x) = j.\omega.\begin{pmatrix} L_1 & M_{12}(z,x) \\ M_{12}(z,x) & L_{p2} \end{pmatrix} \quad (6)$$

This matrix is transformed into the hybrid matrix h with the following relation:

$$h(f,z,x) = \begin{pmatrix} h_{11} & h_{12} \\ h_{21} & h_{22} \end{pmatrix} = \frac{1}{Z_{22}(f)}\cdot\begin{pmatrix} \det Z(f,z,x) & Z_{12}(f,z,x) \\ -Z_{12}(f,z,x) & 1 \end{pmatrix} \quad (7)$$

$$h(f,z,x) = \begin{pmatrix} j\cdot\omega\cdot\dfrac{L_1L_{p2} - M_{12}(z,x)^2}{L_{p2}} & \dfrac{M_{12}(z,x)}{L_{p2}} \\ -\dfrac{M_{12}(z,x)}{L_{p2}} & \dfrac{1}{jL_{p2}\omega} \end{pmatrix} \quad (8)$$

The hybrid matrix H(f,z,x) of the full quadripole can now be computed:

$$H(f,z,x) = \begin{pmatrix} H_{11} & H_{12} \\ H_{21} & H_{22} \end{pmatrix} \quad (9)$$

$$H(f,z,x) = \begin{pmatrix} h_{11}(f,z,x) + R_{sL_1} + \dfrac{1}{jC_1\omega} & h_{12}(f,z,x) \\ h_{21}(f,z,x) & h_{22}(f,z,x) + jC_2\omega + \dfrac{1}{R_2} \end{pmatrix} \quad (10)$$

ASSOCIATION BETWEEN A SOLENOID AND AN ARCHIMEDES COIL

Many different combinations of two given coil geometries have been studied in terms of stability and mutual inductance, including simple geometries such as two circular coils and more complex ones such as two solenoids, a circular coil and an Archimedes coil, and a solenoid and an Archimedes coil (Chaoui *et al*., 2002; 2003a). The objective is to demonstrate experimentally

which case presents a maximum mutual inductance (Chaoui *et al*., 2003a). Indeed, within the literature (Chaoui *et al*., 2002; 2003a; 2003b), the case of two Archimedes coils is adopted as an optimal case since it presents a remarkable mutual inductance. However, through rigorous calculations (Chaoui *et al*., 2003c), better stability can be obtained with two solenoids than with two Archimedes coils, only with a slight drop-off of the mutual inductance. To sum up, it has been shown that a good trade-off between stability and mutual inductance is achieved through the use of an Archimedes coil and a solenoid.

Principle of an inductive link: For stability reasons, it has been demonstrated that the receiver radius b must be lower than the transmitter radius a. Figure 3a shows the representation of the association between a solenoid and an Archimedes coil, while Fig. 3b displays the structure of an Archimedes coil.

The case of a solenoid as an emitter and an Archimedes coil as a receiver presents a remarkable stability and a slightly less pronounced mutual inductance than that of the opposite case. Moreover, it should be noted that an Archimedes coil (surface) is simpler to implant in the human body than a solenoid (in volume).

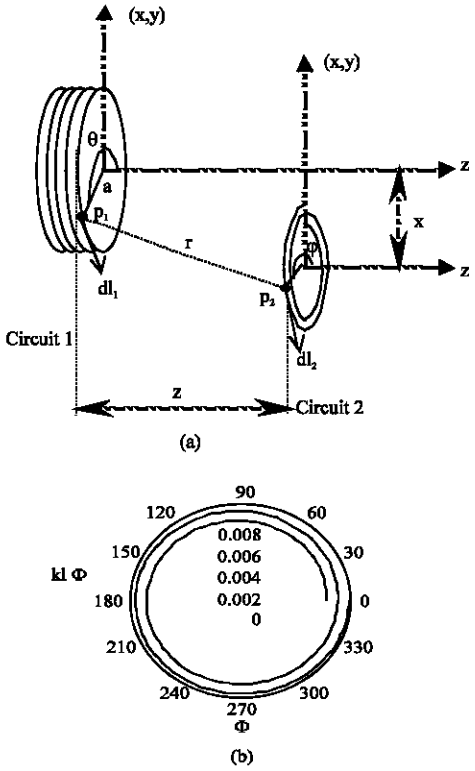

Fig. 3: Layout of a solenoid (radius a) and Archimedes coil (radius b) distant from z longitudinally and x laterally

The mutual inductance of two loop-shaped air coils whose axes are parallel (radius a for emitter and external radius b for receiver, coil distance z, distance between the axes x) can be expressed by the double integral of Neumann's equation:

$$M_{12} = \frac{\mu_0}{4\pi}\int_1\int_2 \frac{\vec{dl_1}\vec{dl_2}}{r} \qquad (11)$$

in which, by replacing the Cartesian coordinates of points P_1 and P_2 and their elementary displacements dl_1 and dl_2, the solved equation of the mutual inductance can be obtained:

$$M_{12}(z,x) = \sum_{i=0}^{N1-1} \frac{\mu_0}{4\pi} \int_{10.2\pi}^{15.2\pi} \int_0^{2\pi} \frac{ar_2(\sin(\phi-\theta)+\phi\cos(\theta-\phi))\ d\theta\ d\phi}{\sqrt{\left(x^2+a^2+(r_2\phi)^2+\left(z+\frac{E}{2}+iE\right)^2\right.}} \qquad (12)$$
$$\left.+2(r_2\phi)x\ \cos\ \phi-2ax\ \cos\ \theta-2a(r_2\phi)\ \cos(\theta-\phi)\right)$$

E is the wire gauge, only considered in the rigorous calculation of the mutual inductance; an experimental measurement of this gauge was performed in (Hochmair, 1984; Leclair, 1992; Chaoui *et al*., 2003a). N_1 is the number of turns of the solenoid.

This equation of the mutual inductance is the one which will be used in the voltage gain and power yield formulae in the next sections. It takes into account the relative locations of the turns, instead of multiplying the result obtained for one turn by the number of turns, as in previous literature.

The longitudinal displacement z should vary between 4 and 8 mm (spacing including the biological tissue and the protective envelope), whereas the lateral displacement should vary between 0 and 10 mm, corresponding to average displacements due to the relative locations of the transmitter system and the receiver.

Computed and practical results of the mutual inductance: In order to highlight the stability of the mutual inductance as a function of lateral displacement, simulation results and measurements will be considered for a 5-turn, 15-mm radius solenoid and a 2-turn, 10-mm outer radius Archimedes coil.

Figure 4 depicts the mutual inductance $M_{12}(z,x)$ as a function of the lateral displacement x for various

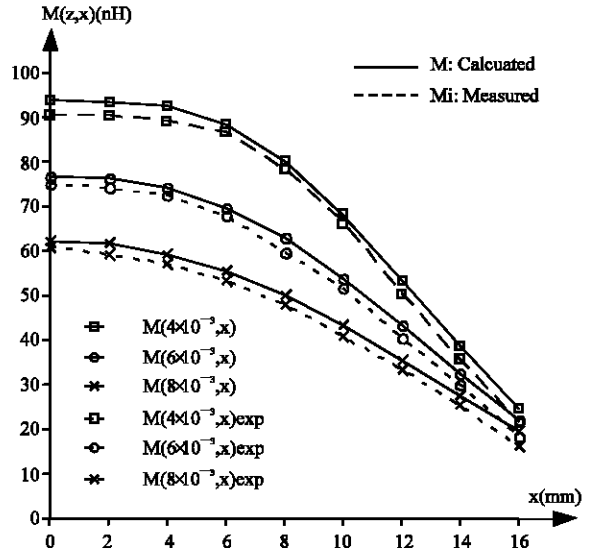

Fig. 4: Mutual inductance between a solenoid (emitter) and an Archimedes coil (receiver) vs. Lateral displacement for various longitudinal displacements

longitudinal displacements z = 4, 6 and 8 mm. This is very close to the real-world case (cochlear implant) in which z is almost a constant from patient to patient (6 mm: mean thickness of biological tissues). It can be noted that angular misalignments are not a concern for a cochlear implant, as demonstrated in (Zierhofer and Hochmair, 1996).

An inductance is purely described by its own geometry, while the mutual inductance is described by the interaction between several geometries, mainly by their relative separation (x and z) and the permeability of the environment in between. This proportionality can be expressed by the coupling coefficient, designated by k.

In general, the coupling coefficient k(z,x) between two magnetically coupled coils is defined by:

$$k(z,x)=\frac{M_{12}(z,x)}{\sqrt{L_1L_2}} \tag{13}$$

in which L_1 is the primary (external) winding inductance and L_2 is the secondary (internal) winding inductance.

The models of the transmitter and receiver coils are respectively a series and a parallel L-R circuit whose values are listed in Table 1, for a 10 MHz operating frequency. The reason why this frequency was chosen is the trade-off between the power absorption in biological tissues (which increases with frequency and is minimal between 7 and 20 MHz) and the transmission frequency (which has to be high enough for our application). Therefore, a 10 MHz frequency ensures a 0.625 S m^{-1} measured conductivity and a 21.6 cm penetration depth.

From this Table 1 and Eq. 12 results between 0.1 and 0.3 are typically obtained for k(z,x).

Stability of the mutual inductance: The complex expression of the mutual inductance depends on several parameters. It is thus important to identify its sensitivity to these variables. As far as lateral displacements are concerned, and with the external radius a of the solenoid and the longitudinal displacement z kept constant, the sensitivity can be expressed by:

$$S=\frac{\Delta M}{\Delta D}/a=cst,z=cst \tag{14}$$

in which ΔM is the variation of the mutual inductance and ΔD the variation of the lateral displacement. The determination of the sensitivity then requires the calculation of the partial derivative of the mutual inductance with respect to the lateral displacement. This can be achieved only if the denominator in Eq 12 is not equal to zero at the boundaries of the integral; in this case, this requirement is met since z represents the spacing encompassing the biological tissues and the protective envelope. It is then possible to express the sensitivity by:

$$S=\left|\frac{\partial M}{\partial x}\right|/a=cst,z=cst \tag{15}$$

The computation of this derivative looks difficult at first glance because of the elliptic integrals in the mutual inductance. However, with a, b and z being constant, the derivation can be performed within the integral (Chaoui *et al*., 2003b), leading to:

$$\sum_{i=0}^{N1-1}\frac{\mu_0}{4\pi}\int_{10.2.\pi}^{15.2\pi}\int_{0}^{2\pi}\frac{\left(x+\left(r_2\phi\right)\cos\phi-a\cos\theta\right)\,d\theta\quad d\phi}{\sqrt{\begin{array}{l}x^2+a^2+\left(r_2\phi\right)^2+\left(z+\dfrac{E}{2}+iE\right)^2+\\ 2\left(r_2\phi\right)x\quad\cos\phi-2ax\\ \cos\theta-2a\left(r_2\phi\right)\quad\cos(\theta-\phi)\end{array}}} \tag{16}$$

This equation has no analytical solution; its resolution is thus achieved through numerical computing. The corresponding results for the mutual inductance are presented below for a 15 mm radius solenoid and a 10 mm radius Archimedes coil.

Figure 5 plots the sensitivity S(z, x) versus the lateral displacement x for various longitudinal displacements z = 4, 6 and 8 mm. These computations do not provide any information on the real value of the mutual inductance. However, other computations performed for several b radii demonstrated that the smaller the radius b, the more stable (and the lower) the mutual inductance.. At the same time, the sensitivity increases for small radii because of the steep increase in the coupling factor for low longitudinal displacements z.

For longitudinal displacements up to 10 mm, the coupling factor k(z,x) varies between 0.1 and 0.3 for various lateral displacements (0-8 mm). This k range is used in the majority of the literature, in which mutual inductance is often represented as a fixed value independent of displacements and coil shapes. Conversely, in this study, this mutual inductance is represented by expression (12) which takes into account both displacements and the optimal shapes of both coils. It can be noted that the stability increases until x = 12 mm, which explains the stability of the voltage gain around the operating frequency, as shown later.

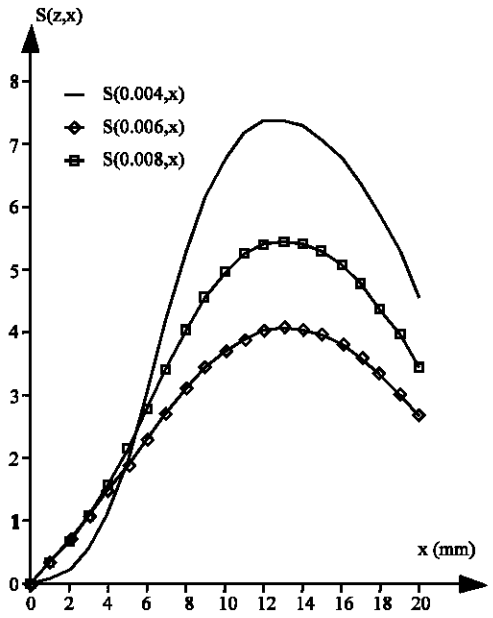

Fig. 5: Sensistivity of the mutal inductance to lateral displacement (in nH/mm) for a 15 mm radius solenoid and a 10 mm radius Archimedes coil

EFFECT OF THE REFLECTED IMPEDANCE

In order to calculate the power Pin, the secondary winding must be reflected to the primary one. Fig. 6 shows the diagram of the equivalent circuit.

The equivalent impedance $Z_{in}(f,z,x)$ seen at the transmitter antenna can thus be written as:

$$Z_{in}(f,z,x)=\frac{V_{in}}{I_1}=\frac{\det(H(f,z,x))}{h_{22}}=R(f,z,x)+j\omega L(f,z,x) \quad (17)$$

Since the current in the secondary is equal to zero, and by taking into account (8) and (10), the resistance and the inductance can be calculated:

$$R(f,z,x)=R_1+R_{L1}+\frac{M(z,x)^2}{L_2^{\,2}}\frac{1}{1+\left[Q_r\frac{\omega_r}{\omega}((\frac{\omega}{\omega_r})^2-1)\right]^2}R_2 \quad (18)$$

$$L(f,z,x)=L_1\left[1-\frac{M(z,x)^2}{L_1L_2}\right]-\frac{\frac{M(z,x)^2}{L_2}Q_r^2(\frac{\omega_r}{\omega})^2\left[(\frac{\omega}{\omega_r})^2-1\right]}{1+\left[Q_r\frac{\omega_r}{\omega}((\frac{\omega}{\omega_r})^2-1)\right]^2} \quad (19)$$

in which R(f,z,x) and L(f,z,x) represent the equivalent resistance and the equivalent inductance due to the inductive coupling, respectively. Q_r and ω_r are the quality factor and the pulsation of the receiver resonant circuit, respectively

$$Q_r=R_2C_p\omega_r \quad (20)$$

$$\omega_r=\frac{1}{\sqrt{L_{p2}C_p}} \quad (21)$$

Figure 7a and b show respectively the reflected resistance and inductance with no lateral displacement and a quality factor equal to 32 at the receiver.

A quadratic dependency of the reflected impedance with respect to the coupling between both coils can be observed. Moreover, this coupling decreases quickly with an increase in distance.

LOAD EFFECT ON THE VOLTAGE GAIN

The most influential parameters on the voltage gain are the geometrical shapes, their environment, and mainly the lateral displacement caused by the misplacement of the external part with respect to the internal part of the system. In fact, the reflected load resistance also depends on displacements.

Using Eq. 22 and 23:

$$V_1(f,z,x)=H_{11}(f,z,x)I_1+H_{12}(f,z,x)V_2 \quad (22)$$

$$I_2(f,z,x)=H_{21}(f,z,x)I_1+H_{22}(f,z,x)V_2 \quad (23)$$

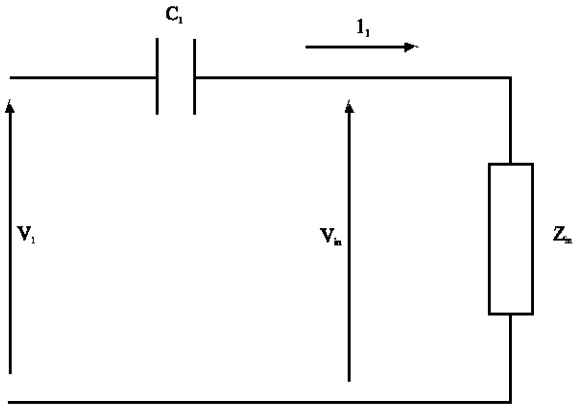

Fig. 6: Equivalent circuit of the inductive link reflected to the primary winding

and seeing that there is no current in the secondary winding, the voltage gain of the inductive link can thus be obtained:

$$G_v(f,z,x)=\frac{V_2}{V_1}=\left|\frac{H_{21}(f,z,x)}{detH(f,z,x)}\right| \quad (24)$$

For a 6 mm longitudinal displacement z (average spacing encompassing the biological tissues and the protective envelope) or a 4 mm lateral displacement x, $G_v(f,z,x)$ is plotted in Fig. 8 and Fig. 9 as a function of frequency for various load resistances and longitudinal displacements, respectively.

This function is as function of the different displacements, but not for various coupling factors. The calculation is based on circuit experimental parameters summarized in Table 1. These values are also used for the following plots.

Figure 8 shows that, for a zero lateral displacement, the maximum voltage gain is achieved in a frequency range between 9.5 and 10.5 MHz. Within this range, the voltage gain changes slightly with the load resistance, with a remarkable stability for x between 0 and 12 mm, while the bandwidth decreases at the same time.

Figure 9 demonstrates that the maximum voltage gain is achieved within the same frequency range, for x = 0, Q_r = 32 and R_{Load} = 1 kΩ. Within this region, the voltage gain changes for x = 4, 6, 8 and 10 mm. Beyond, the voltage gain G(f,z,x) decreases with x increasing. This is an expected result, since the more the transmitter moves away from the receiver, the more the voltage gain decreases.

The voltage gain increases with z within the passband, while the bandwidth itself decreases at the same time; the same phenomenon can be observed for x.

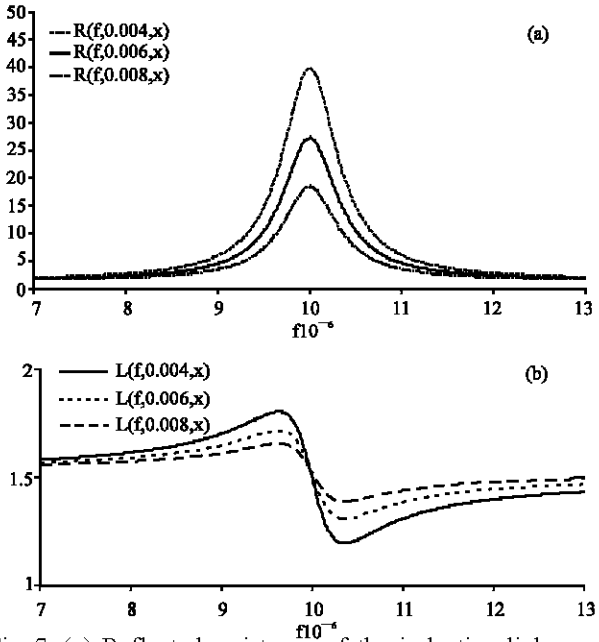

Fig. 7: (a) Reflected resistance of the inductive link vs. frequency for various longitudinal displacements, Qr = 32 and Rload = 1 kΩ
(b) Reflected inductance of the inductive link vs.

Moreover, both peak values of the voltage gain increase with Q_e. Conversely, when Q_e and/or Q_r decrease, the voltage gain becomes plateau-shaped, with a slight reduction of the amplitude and no peaks.

LOAD EFFECT ON THE POWER YIELD

The yield, i.e., the ratio between the power delivered to the receiver circuit and the overall power consumption, is given by:

$$\eta=\frac{P_{out}}{P_{in}} \quad (25)$$

thus, the power yield will be

$$\eta(f,z,x)=\frac{P_{out}}{P_{in}}=\frac{V_2^2}{2R_{Load}}\frac{2R(f,z,x)}{V_R^2} \quad (26)$$

in which V_R is the voltage across R(f,z,x).
By neglecting R_1 within the computation and inserting $G_R = V_R|V_1$ into the yield (18) this leads to:

$$G_R(z,x,\omega)=\frac{R(z,x,\omega)}{R(z,x,\omega)+j\omega L(z,x,\omega)+\frac{1}{j\omega C_1}} \quad (27)$$

The power yield is then given by:

$$\eta(z,x,\omega)=\left|\frac{G_v}{G_R}\right|^2\frac{R(z,x,\omega)}{R_{Load}} \quad (28)$$

Table 1: Specifications of the circuits of emission and reception

Coil shape	Emitter Coil Solenoid	Receiver Coil Archimede's Turns
Number of Turns	5	2
Diameter	30 mm	20 mm
Inductance at 10 MHz	1.54 µH	198.45 nH
Series resistance at 10 MHz	0.527 Ω	0.361 Ω

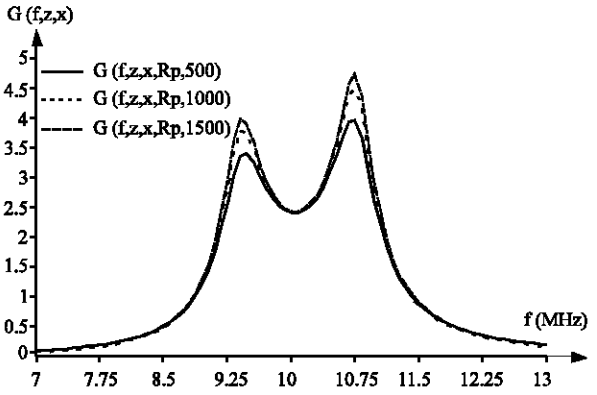

Fig. 8: Voltage gain vs. frequency for various loads, longitudinal displacement z = 6 mm, lateral displacement x = mm, Q_r = 32

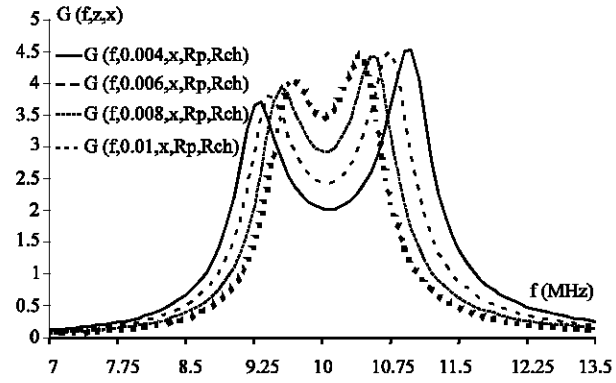

Fig. 9: Votage gain vs. frequency for various longitudinal displacements, lateral displacement x = 0 mm, Q_r = 32 and R_{load} = 1 kΩ

This demonstrates that the highest yield is obtained when the output impedance of the source matches the one of the network.

This yield depends on k, which itself depends on lateral and longitudinal displacements. Figure 10 plots the power yield as a function of lateral displacement x, while Fig. 11 plots this yield as a function of coil distance z. These calculations are based on circuit specifications in Table 1 and the relationship M(z,x) in Fig. 4. In this case, the computation of ç is based on a coil distance z derived from a solenoid and an Archimedes coil with radii a and b (b<a).

It can be seen that this yield is independent from coupling for a coil distance up to z = 8 mm and a lateral displacement x = 8 mm. Moreover, it is almost independent from x until x = 10 mm. This high stability is mainly due to the proper choice of both coil geometries. Figure 12 demonstrates that a steep improvement of the overall power yield can be obtained. Within the frequency range (between 9.5 and 10.5 MHz), the optimal global yield varies between 55 and 63% for z = 6 mm, with only a slight reduction with Q_p or Q_s.

CONCLUSIONS

This article shows that the mutual inductance M (and consequently the coupling factor k) of two coupled coils can be determined as a function of lateral and longitudinal displacements, provided that the inductances and quality factors of both the primary and secondary coils are well known and that the secondary load is also pre-defined. Once these displacements are known, the exact magnetic field required to meet power constraints can be computed, which leads to the gain and the power yield of the system. Moreover, the geometries presented in this article, i.e. the combination between a solenoid and an Archimedes coil, are well-suited for implantable systems thanks to their high stability and low sensitivity to misalignments.

The method described in this paper does not require any knowledge of the coupling itself, but only the two-dimensional displacements, which leads to a simple computation of the mutual inductance M(f,z,x), though at the expense of complexity as far as the voltage gain and power yield are concerned. Obviously, this concept can be used when reasonably high coupling factors apply, hence the reflected impedance Z(f,z,x) is measurable.

The R(f,z,x) and L(f,z,x) formulae should then be implemented within an electric simulator, which may output the real-world time-domain signals of an implantable system as a function of displacements, leading to the electrical verification of this system. This should lead to an evaluation of the efficiency of bi-directional data transmission. For that purpose, the use of the VHDL-AMS language is being investigated.

REFERENCES

Catryasse, M., B. Hermans and R. Puers, 2004. An inductive power system with integrated bi-directional data-transmission, ELSEVIER Sensors and Actuators A 115, pp: 221-229.

Chaoui, M., H. Ghariani, M. Lahiani and F. Sellami, 2002. Maximum of mutual inductance by inductive link. The 14th IEEE Intl. Conference on Microelectronics ICM2002, pp: 265-268.

Chaoui, M., H. Ghariani, M. Lahiani and F. Sellami, 2003a. Optimization of the output of energy transfer in the system implantabless. The 7th IEEE Intl. Conference on Intelligent Engineering Systems: INES 2003, Assiut Luxor, Egypt, pp: 572-575.

Chaoui, M., H. Ghariani, M. Lahiani and F. Sellami, 2003b. Stability of the mutual inductance in the implantable systems. The First Annual Northeast Workshop on Circuits and Systems: NEWCAS 2003, Montreal, Canada.

Chaoui, M., H. Ghariani, M. Lahiani and F. Sellami, 2003c. Experimental results of the mutual inductance between various coils for the transmission of the energy and the information: Application implantable system Sciences of Electronic, Technology of Information and Telecommunication: SETIT 2003, Sousse, Tunisia, pp: 85.

Galbraith, D.C., M. Soma and R.L. White, 1987. A wide-band efficient inductive transdermal power and data link with coupling insensitive gain. IEEE Transactions on Biomedical Engin., 34: 265-275.

Hochmair, E.S., 1984. System optimisation for improved accuracy transcutaneous signal and power transmission. IEEE Transactions on Biomedical Engin., 31: 177-186.

Leclair, M., 1992. Characterization of an inductive link intended to pass current and data to an implantable stimulator. Memory of thesis Sherbrooke (Quebec) Canada.

Muñoz, R., L. Leija, J. Flores, J.A. Alvarez., A. Minor and J.L. Reyes, 2000. Study of a transcutaneous inductive link for transmission of energy in an electronic implantable device., 21: 129-136

Soma, M., D.C. Galbraith and R.L. White, 1987. Radio-frequency coils in implantable devices: Misalignment analysis and design procedure. IEEE Transactions on Biomedical Engin., 24: 276-282.

Zierhofer, C.M. and E.S. Hochmair, 1996. Geometric approach for coupling enhancement of magnetically coupled coils. IEEE Transactions on Biomedical Engin., 43: 708-714.

Zierhofer, C.M. and E.S. Hochmair, 1990. High-efficiency coupling-insensitive transcutaneous power and data transmission via an inductive link. IEEE Transactions on Biomedical Engin., 37: 716-722.